J. Phys. Chem. A **2007,** *111,* 2283−2292

Unimolecular Reactions of Vibrationally Excited $CF_2ClCHFCH_3$ and $CF_2ClCHFCD_3$: Evidence for the 1,2-FCl Interchange Pathway

M. O. Burgin,[†] J. G. Simmons Jr.,[†] G. L. Heard,[†] D. W. Setser,[‡] and B. E. Holmes*,[†]

Department of Chemistry, The University of North Carolina at Asheville, One University Heights, Asheville, North Carolina 28804-8511, and Department of Chemistry, Kansas State University, Manhattan, Kansas 66506

Received: October 12, 2006; In Final Form: January 18, 2007

Chemically activated $CF_2ClCHFCH_3$ and $CF_2ClCHFCD_3$ molecules were prepared with 94 kcal mol^{-1} of vibrational energy by the recombination of CF_2ClCHF and $CH_3(CD_3)$ radicals at room temperature. The unimolecular reaction pathways were 2,3-FH(FD) elimination, 1,2-ClF interchange and 1,2-ClH elimination; the interchange produces $CF_3CHClCH_3(CF_3CHClCD_3)$ with 105 kcal mol^{-1} of vibrational energy. Rate constants for $CF_2ClCHFCH_3$ [$CF_2ClCHFCD_3$] were $(3.1 \pm 0.4) \times 10^6$ s^{-1} [$(1.0 \pm 0.1) \times 10^6$ s^{-1}] for 2,3-FH [FD] loss, $(1.5 \pm 0.2) \times 10^6$ s^{-1} [$(8.3 \pm 0.9) \times 10^5$ s^{-1}] for 1,2-ClF interchange, and $(8.2 \pm 1.0) \times 10^5$ s^{-1} [$(5.3 \pm 0.6) \times 10^5$ s^{-1}] for 1,2-ClH [DCl] loss. These correspond to branching fractions of 0.55 ± 0.06 [0.43 ± 0.04] for 2,3-FH [FD] loss, 0.29 ± 0.03 [0.35 ± 0.04] for 1,2-ClF interchange, and 0.16 ± 0.02 [0.22 ± 0.02] for 1,2-ClH [ClD] loss. Kinetic-isotope effects were 3.0 ± 0.6 for 2,3-FH [FD] loss, 1.6 ± 0.3 for 1,2-ClH loss, and 1.8 ± 0.4 for 1,2-ClF interchange. The $CF_3CHClCH_3$ ($CF_3CHClCD_3$) molecules formed by 1,2-FCl interchange react by loss of HCl [DCl] with rate constants of $(5.6 \pm 0.9) \times 10^7$ s^{-1} [$(2.1 \pm 0.4) \times 10^7$] s^{-1} for an isotope effect of 2.7 ± 0.4. Density functional theory was employed to calculate vibrational frequencies and moments of inertia for the molecules and for the transition-state structures. These results were used with RRKM theory to assign threshold energies from comparison of computed and experimental unimolecular rate constants. The threshold energy for ClF interchange is 57.5 kcal mol^{-1}, and those for HF and HCl channels are 2−5 kcal mol^{-1} higher. Experiments with vibrationally excited $CF_2ClCF_2CF_3$, $CF_2ClCF_2CF_2Cl$, and CF_2ClCF_2Cl, which did not show evidence for ClF interchange, also are reported.

1. Introduction

The unimolecular reactions of a series of chlorofluoropropane molecules are being systematically investigated by this laboratory using chemical activation techniques coupled with electronic structure calculations.[1−6] The vibrational frequencies and moments of inertia of the transition state and molecule, which are obtained from density-functional theory (DFT) calculations, were employed with statistical RRKM theory to calculate unimolecular rate constants for FH and ClH elimination. Comparison of the experimental and calculated unimolecular rate constants permits assignment of threshold energies. The $CF_2ClCHFCH_3(CD_3)$ molecule was selected in the present study because DFT calculations[4] had suggested the 1,2-ClF interchange would be competitive with 4-centered HX (X = F or Cl) elimination reactions. Threshold energies are assigned for 1,2-FCl interchange, 1,2-ClH elimination and 2,3-FH elimination from $CF_2ClCHFCH_3$, as well as for 2,3-ClH elimination from $CF_3CHClCH_3$. The $CF_2ClCHFCH_3(CD_3)$ molecules, which were generated by the recombination of CF_2ClCHF and $CH_3(CD_3)$ radicals, have 94 kcal mol^{-1} of vibrational energy in a bath gas at room temperature. The $CF_2ClCHFCD_3$ data are used to confirm the results from $CF_2ClCHFCH_3$.

We previously measured rate constants, kinetic-isotope effects, and branching ratios for the unimolecular reactions of chemically activated $CF_2ClCF_2CH_3$ and $CF_2ClCF_2CD_3$ molecules.[4,5] The observed products were $CF_2ClCF{=}CH_2$ ($CF_2ClCF{=}CD_2$) from 2,3-FH elimination and $CF_3CF{=}CH_2$ ($CF_3CF{=}CD_2$) from Cl−F interchange followed by 2,3-ClH elimination. The kinetic-isotope effect, k_{FH}/k_{FD}, for the 2,3-FH/FD elimination was 2.9, which is comparable to isotope effects for other direct HF/DF or HCl/DCl elimination reactions from molecules with ≈95 kcal mol^{-1} of energy.[1,3,7−9] For example, the isotope effects are $CF_3CFClCH_3/CF_3CFClCD_3$[3] = 2.0 ± 0.2, CF_3CH_3/CF_3CD_3[3] = 3.0 ± 0.1, CF_2ClCH_3/CF_2ClCD_3[7] = 3.0 ± 0.9, and C_2H_5Cl/C_2D_5Cl[9] = 3.3 ± 0.4. However, k_{ClH}/k_{ClD} was only 1.5 for the interchange process. The small isotope effect suggested that the rate-limiting step did not involve rupture of the C−H/C−D bond. On the basis of electronic structure calculations, a rate-limiting 1,2-ClF interchange reaction to give $CF_3CFClCH_3$, followed by a rapid 2,3-ClH elimination reaction, was proposed.[4,5] The ClH and FH-elimination reactions from $CF_3CFClCH_3(CD_3)$ now have been independently characterized, and the fast HCl-elimination reaction has been confirmed.[3]

As described above,[5] the interchange product, $CF_3CFClCH_3(CD_3)$, from $CF_2ClCF_2CH_3(CD_3)$ could not be experimentally detected.[5] In search of direct evidence for 1,2-ClF interchange reactions, we selected $CF_2ClCHFCH_3(CD_3)$ for study in anticipation that $CF_3CHClCH_3(CD_3)$ might be observed. The presence of the β-H atom is an asset, because additional HX elimination pathways are possible and threshold energies are lowered for the interchange and for the HX elimination reactions. Furthermore, the faster absolute decomposition rate for $CF_2ClCHFCH_3$ might enable experiments to be run at higher bath gas pressure, which could permit the interchange product, $CF_3CHClCH_3$, to be collisionally stabilized.

[†] The University of North Carolina at Asheville.

[‡] Kansas State University.

10.1021/jp066722f CCC: $37.00

In fact, $CF_3CHClCH_3(CD_3)$ was observed, and the 1,2-ClF interchange reaction has been proven. A Cl−F interchange reaction also has been proposed to explain the products from the decomposition of CF_2HCH_2Cl.[10,11] and CF_3CH_2Cl.[10,12a] On the other hand, ClF interchange was not observed in experiments to be reported here for chemically activated $CF_2ClCF_2CF_3$, $CF_2ClCF_2CF_2Cl$, and CF_2ClCF_2Cl. Although the structural factors that affect the threshold energy for Cl−F interchange in chlorofluoroalkanes have not been fully identified, the interchange reaction frequently can compete with HF and HCl elimination or rupture of C−Cl bonds.

The $CF_2ClCHFCH_3$ molecules were prepared from photolysis of $CF_2ClCHFI$ and CH_3I mixtures. Reactions 1−3 are the expected combination and disproportionation processes.

$$\cdot CH_3 + \cdot CH_3 \xrightarrow{k_c} CH_3CH_3 \tag{1}$$

$$2\cdot CHFCF_2Cl \xrightarrow{k_c} CF_2ClCHFCHFCF_2Cl^* \tag{2a}$$

$$\xrightarrow{k_d} CF_2{=}CHF + CF_2ClCHFCl \tag{2b}$$

$$\cdot CHFCF_2Cl + \cdot CH_3 \xrightarrow{k_c} CF_2ClCHFCH_3^* \tag{3a}$$

$$\xrightarrow{k_d} CF_2{=}CHF + CH_3Cl \tag{3b}$$

A similar set of combination and disproportionation reactions can be written for the $CF_2ClCHF + CD_3$ system. Because the product of reaction 2a has two chiral carbons, both *meso*- and *d,1*-stereoisomers are formed. At the pressures of these experiments, $(CF_2ClCHF)^*_2$ is stabilized by collisions. The absence of any product that could be associated with CF_3CHCl radicals precluded the possibility that the CF_2ClCHF radical rearranged prior to reactions 2 and 3. Vibrationally excited $CF_2ClCHFCH_3^*$ can eliminate HF (reactions 4a and 4c) or HCl (reaction 4b), interchange Cl−F (reaction 4d), or be collisionally stabilized (reaction 5). The 1,2-ClF interchange is about 10 kcal mol^{-1}

$$CF_2ClCHFCH_3^* \xrightarrow{k_{1,2-FH}} \text{Z- and E-}CFCl{=}CFCH_3 + HF \tag{4a}$$

$$\xrightarrow{k_{1,2-ClH}} CF_2{=}CFCH_3 + HCl \tag{4b}$$

$$\xrightarrow{k_{2,3-FH}} CF_2ClCH{=}CH_2 + HF \tag{4c}$$

$$\xrightarrow{k_{1,2-ClF}} CF_3CHClCH_3^* \tag{4d}$$

$$\xrightarrow{k_M[M]} CF_2ClCHFCH_3 \tag{5}$$

exoergic,[4] and the $CF_3CHClCH_3^*$ molecules will eliminate HCl or be stabilized by collisions:

$$CF_3CHClCH_3^* \xrightarrow{k_{2,3-ClH}} CF_3CH{=}CH_2 + HCl \tag{6}$$

$$\xrightarrow{k_M[M]} CF_3CHClCH_3 \tag{7}$$

The reverse isomerization and 1,2-FH elimination are not competitive with reaction 6. The unimolecular rate constants are obtained from plots of the ratio of the experimental yield of the decomposition (D_i) and stabilization (S) products versus inverse pressure for each activated molecule. Collisional deactivation is efficient for the $CH_3I/CF_2ClCHFI$ bath gas mixture, i.e., the unit deactivation assumption, so that the slope of these plots provide limiting high-pressure rate constants.[1]

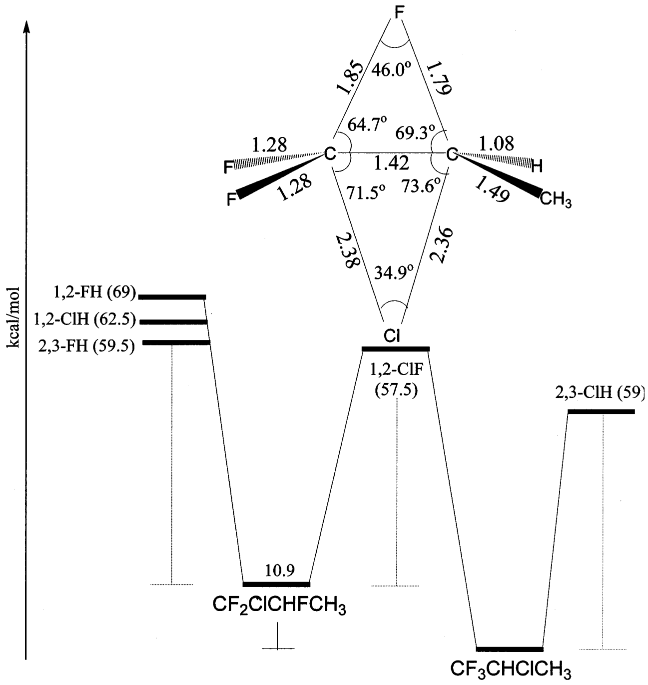

Figure 1. Schematic representation of the threshold energies for the various unimolecular processes. The differences in threshold energies have been exaggerated for clarity of presentation. The average energy of the initially formed $CF_2ClCFHCH_3$ molecules is 94.3 kcal mol^{-1} and the energy of the rearranged $CF_3CHClCH_3$ molecules is 104.8 kcal mol^{-1}. The structure of the transition state for 1,2-ClF interchange also is shown (the C−C distance is 0.11 Å shorter than for $CF_2ClCHFCH_3$); see Figure 1 of ref 4 for the transition state of $CF_2ClCF_2CH_3$.

A schematic overview of the unimolecular processes is presented in Figure 1. The relative rates of the reactions are mainly governed by their threshold energies, E_0. We followed the same procedure that has been adopted in previous work[1−3] to assign E_0 for the unimolecular reactions. Electronic structure calculations from DFT are used to obtain moments of inertia and vibrational frequencies of the molecules and transition states. Thus, the threshold energy is the only undetermined variable in the RRKM calculation, and it can be assigned from matching the calculated and experimental rate constants. The E_0 values cited in Figure 1 are our assigned values. The threshold energies for reactions of $CF_2ClCHFCH_3$ will be compared to those from $CF_2ClCF_2CH_3$ in the Discussion with emphasis on characterization of the ClF interchange reactions. This study also provides additional insight[6] into the nature of 1,2-X′H and 2,3-XH elimination transition states of CX'_3CHXCH_3 (X, X′ = F or Cl) type molecules.

2. Experimental Section

Pyrex vessels with volumes ranging from 19.8 to 564.9 cm^3 containing 1.22 μmoles of methyl iodide or methyl iodide-d_3 with 1.22 μmol of 1-chloro-2-iodo-1,1,2-trifluoroethane, plus small amounts of mercury and mercury(I) iodide were photolyzed with a high-pressure 200 W mercury lamp at room temperature. The presence of mercury(I) iodide in the vessels during photolysis aids formation of $CH_3(CD_3)$ and CF_2ClCHF radicals. Photolysis times, which depended upon the size of the vessel, were between 2 and 7 min. About 30% of the $CF_2ClCHFI$ and 5% of the CH_3I were photolyzed. All gas samples were prepared on grease-free vacuum lines; an MKS 270C

TABLE 1: Mass Spectral Data at 70 eV (*m*/*e*, Relative Abundance and Assignment)

$CF_3CH{=}CH_2$			$CF_3CH{=}CD_2$		
m/*e*	RA	assignment	*m*/*e*	RA	assignment
27	100	$C_2H_3^+$	29	100	$C_2HD_2^+$
95	97	$C_3F_3H_2^+$	98	83	$C_3F_3D_3^+$
96	89	$C_3F_3H_3^+$	96	55	$C_3F_3HD^+$
51	40	CF_2H^+	97	49	$C_3F_3D_2^+$
69	38	CF_3^+	48	42	$C_2FHD_2^+$
46	37	$C_2FH_3^+$	79	35	$C_3F_2HD_2^+$

$CF_2ClCH{=}CH_2$			$CF_2ClCH{=}CD_2$		
m/*e*	RA	assignment	*m*/*e*	RA	assignment
77	100	$C_3F_2H_3^+$	79	100	$C_3F_2HD_2^+$
51	50	CF_2H^+	29	31	$C_2HD_2^+$
27	32	$C_2H_3^+$	51	27	CF_2H^+
31	18	CF^+	97	26	$C_2F_2{}^{35}Cl^+$
26	12	$C_2H_2^+$	52	23	CF_2D^+
15	11	CH_3^+	31	18	CF^+

$CF_2ClCHFCH_3$			$CF_2ClCHFCD_3$		
m/*e*	RA	assignment	*m*/*e*	RA	assignment
47	100	$C_2FH_4^+$	50	100	$C_2FHD_3^+;CF_2^+$
27	25	$C_2H_3^+$	100	22	$C_3F_3HD_3^+$
97	14	$C_3F_3H_4^+$	29	18	$C_2HD_2^+$
77	7	$C_3F_2H_3^+$	79	10	$C_3F_2HD_2^+$
45	4	$C_2FH_2^+$	51	9	CF_2H^+
33	4	CFH_2^+	85	8	$CF_2{}^{35}Cl^+$

$CF_3CHClCH_3$			$CF_3CHClCD_3$		
m/*e*	RA	assignment	*m*/*e*	RA	assignment
63	100	$C_2{}^{35}ClH_4^+$	66	100	$C_2{}^{35}ClHD_3^+$
27	99	$C_2H_3^+$	30	69	$C_2D_3^+$
65	31	$C_2{}^{37}ClH_4^+$	68	22	$C_2{}^{37}ClHD_3^+$
77	27	$C_3F_2H_3^+$	69	12	CF_3^+
51	23	CF_2H^+	27	12	C_2HD^+
69	20	CF_3^+	135	11	$C_3{}^{35}ClF_3HD_3^+$

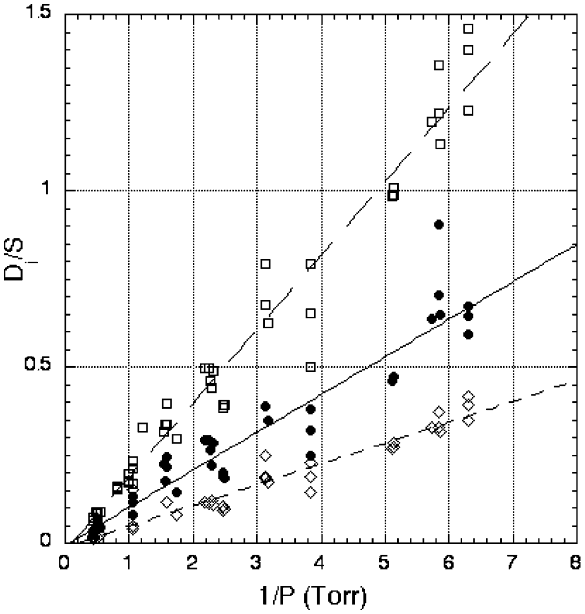

Figure 2. D_i/S versus reciprocal pressure plots for $CF_2ClCHFCH_3$. Squares: 2,3-FH elimination with a slope of 0.22 ± 0.01 Torr, an intercept of −0.02 ± 0.02, and a correlation coefficient of 0.98. Solid circles: 1,2-ClF interchange with a slope of 0.11 ± 0.01 Torr, an intercept of −0.004 ± 0.024, and a correlation coefficient of 0.95. Diamonds: 1,2-ClH elimination with a slope of 0.059 ± 0.004 Torr, an intercept of −0.011 ± 0.016, and a correlation coefficient of 0.96.

electronic manometer was used to measure pressures of CH_3I and $CF_2ClCHFI$. The CH_3I was purchased from Aldrich and $CF_2ClCHFI$ was obtained from PCR (now SynQuest).

Product identification was based on the mass spectral fragmentation pattern obtained from a Shimadzu QP5000 GC/MS equipped with a 105 m Rtx-1 column; see Table 1. It was difficult to obtain a reliable mass spectrum of $CF_2{=}CFCH_3$ ($CF_2{=}CFCD_3$) because this yield was the smallest of the decomposition products. The products from reaction 4b were identified by the presence of the parent ions at *m*/*e* = 96 and 99 for $CF_2{=}CFCH_3$ and $CF_2{=}CFCD_3$, respectively, and by the allyl radical cation at *m*/*e* = 95 and 97 formed by loss of H or D from the parent ion. Agreement also existed with the mass spectra from $CF_2{=}CFCH_3$ and $CF_2{=}CFCD_3$ in ref 6. The temperature program began with an initial temperature of 35 °C for a period of 20 min, followed by a temperature increase at a rate of 2 °C per min until the column reached 100 °C; the heating rate was then increased to a rate of 4 °C per min until the column reached a final temperature of 200 °C. The following products and (typical retention times in minutes) were observed: C_2H_6 and $CHF{=}CF_2$ (8.1 but not resolved) $CF_3CH{=}CH_2$ (8.7), $CF_2{=}CFCH_3$ (9.2), $CF_2ClCH{=}CH_2$ (12.6), $CF_3CHClCH_3$ (13.8), $CF_2ClCHFCH_3$ (14.5), $CF_2ClCHFCl$ (15.9), and *meso*- and *d*,*l*-$CF_2ClCHFCHFCF_2Cl$ (32.6 and 35.8, but the specific diasteroisomer identity is not known). The retention times for $CF_2ClCHFI$ and CH_3I were 20.5 and 29.4 min, respectively. Commercial samples of $CF_3CH{=}CH_2$, $CHF{=}CF_2$, and C_2H_6 were available to confirm the identity of these products. We found no evidence for *Z*- and *E*-$CFCl{=}CFCH_3$ and $CF_2{=}CClCH_3$, which would be products from 1,2-FH elimination from $CF_2ClCHFCH_3$ and $CF_3CHClCH_3$, respectively. The $CF_3CHClCH_3$ is from 1,2-ClF interchange followed by collisional stabilization (reactions 4d plus 7), and $CF_3CH{=}CH_2$ is from 2,3-ClH elimination (reactions 4d plus 6).

Analyses of the reaction mixtures needed for the D_i/S plots were conducted with a Shimadzu GC-14A with a flame-ionization detector. A Shimadzu CR501 Chromatopac Integrator acquired and integrated the area associated with each signal. A Mxt-1 column of 105 m length and 0.53 mm diameter was used with the temperature program cited above. Direct calibration of the response of the flame-ionization detector was impossible, because authentic samples were not available for most of the products. We have found[12b] that relative response factors for halogenated propenes formed by elimination of HCl or HF from corresponding halogenated propanes are nearly unity, and values of 1.0 were adopted for the propanes and propenes of these experiments. Thus, the data points of the D_i/S plots are just the ratios of the areas of the peaks associated with the designated decomposition and stabilization products. The uncertainty of the calibration factors could introduce a 10% uncertainty in the D_i/S ratios and, for the worst case scenario, a 20% uncertainty in the product branching fractions.

3. Results

3.1. Experimental Rate Constants. The results to be presented include the reactions of $CF_3CHClCH_3(CD_3)$ molecules. However, the reactions of $CF_2ClCHFCH_3(CD_3)$ will be considered first. The products from reactions 4b, 4c, and 4d, were detected; the 1,2-FH elimination pathway was not observed. The D_i/S versus (pressure)$^{-1}$ plots, are given in Figures 2 and 3 for $CF_2ClCHFCH_3$ and for $CF_2ClCHFCD_3$. The D_i/S plot for F−Cl exchange was constructed by combining the yields of $CF_3CHClCH_3$ and $CF_3CH{=}CH_2$ to obtain the total rearrangement product. The D_i/S values range from 0 to 1.5 in Figures 2 and 3; these linear plots represent the high-pressure

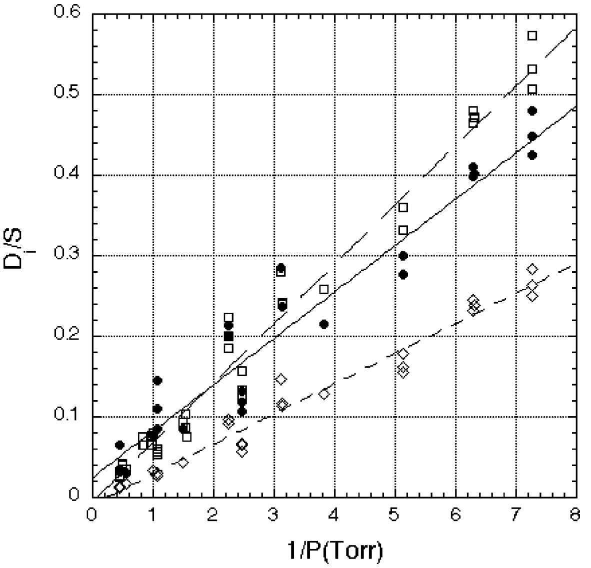

Figure 3. D_i/S versus reciprocal pressure plot for $CF_2ClCHFCD_3$. Squares: 2,3-FD elimination with a slope of 0.074 ± 0.003 Torr, an intercept of −0.006 ± 0.007, and a correlation coefficient of 0.99. Solid circles: 1,2-ClF interchange with a slope of 0.060 ± 0.003 Torr, an intercept of 0.019 ± 0.011, and a correlation coefficient of 0.98. Diamonds: 1,2-ClH elimination with a slope of 0.038 ± 0.002 Torr, an intercept of −0.009 ± 0.006, and a correlation coefficient of 0.99.

region and the slopes correspond to the average rate constants, $k_{\langle E\rangle}$. The intercepts are nearly zero in each case; the slopes from the plots have standard deviations of less than 10%, and the rate constant values should be reliable. The unimolecular rate constants obtained from these data are summarized in Table 2 for $CF_2ClCHFCH_3(CD_3)$.

A plot of the product branching fractions for $CF_2ClCHFCH_3$ is shown in Figure 4. This plot includes two sets of lower pressure points than shown in the D_i/S plots of Figures 2. The average branching fractions are 0.55 ± 0.06, 0.29 ± 0.03, and 0.16 ± 0.02 for 2,3-FH loss, Cl−F interchange, and 1,2-ClH loss, respectively, for $CF_2ClCHFCH_3$. The kinetic-isotope effects for these three processes are 2.97 ± 0.61, 1.83 ± 0.37, and 1.55 ± 0.31, respectively. The largest effect is for 2,3-FH(FD) elimination, which is expected because only this process has a primary kinetic-isotope effect. The uncertainty in the kinetic-isotope effects were calculated from the rate constants in Torr units with ±15% uncertainty. Because of the large kinetic-isotope effect for 2,3-FH elimination, the branching fraction for Cl−F interchange increases to 0.35, that for 1,2-ClH elimination increases to 0.22, and that for 2,3-FD decreases to 0.43 for $CF_2ClCHFCD_3$.

The $CF_3CHClCH_3(CD_3)$ molecules formed by reaction 4d can decompose, in principle, by 1,2-FH or by 2,3-ClH elimination; however, only HCl elimination was observed. The HCl elimination is much faster than the reverse Cl−F interchange process, and the reverse reaction need not be considered. Because a small fraction of the $CF_3CHClCH_3(CD_3)$ molecules were stabilized in the 2.0−0.15 Torr range, a $CF_3CH{=}CH_2(CD_2)/CF_3CHClCH_3(CD_3)$ vs (pressure)$^{-1}$ plot could be constructed. The data of Figure 5 cover the D/S range from 1.5 to 20 for $CF_3CHClCH_3$ and from 1.0 to 12 for $CF_3CHClCD_3$. In this range for D/S, the consequence of cascade deactivation of the vibrationally excited molecules can cause upward curvature in D/S vs (pressure)$^{-1}$ plots.[15,16] The intercepts of −0.24 ± 0.63 and 1.0 ± 0.5 could be from curvature in the plots and/or scatter in the higher pressure data. The collisional deactivation efficiencies for CH_3I and $CF_2ClCHFI$ for vibrationally excited haloethanes or halopropanes have not been measured. If the deactivation is efficient ($\langle E\rangle \geq 10$ kcal mol^{-1} per collision), as expected, then a linear fit to the data of Figure 5 will be a close representation of the high-pressure rate constant. The data for $CF_3CHClCD_3$ probably are the more reliable, because the D/S range is lower. The rate constants based upon a linear fit to the D/S plots in Figure 5 are given in Table 2. These values should be considered as upper limits to the limiting high-pressure rate constants, and we have assigned an uncertainty of ±20% to the rate constants. The kinetic-isotope effect is 2.7 for 2,3-ClH(ClD) elimination, which is typical.[3] The 18-fold larger rate constant for 2,3-ClH

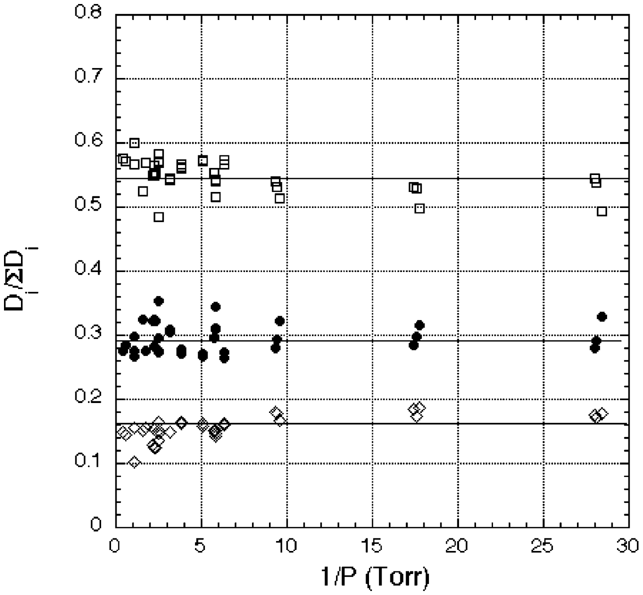

Figure 4. Plot of product branching fractions for the $CF_2ClCHFCH_3$ system vs pressure^{-1}. Squares: fraction for 2,3-FH elimination. Circles: fraction for 1,2-Cl−F interchange. Diamonds: fraction for 1,2-ClH elimination. The products for ClF interchange include the yields of both $CF_3CHClCH_3$ and $CF_3CH{=}CH_2$. The average branching fractions are 0.55 ± 0.05, 0.29 ± 0.03, and 0.16 ± 0.02.

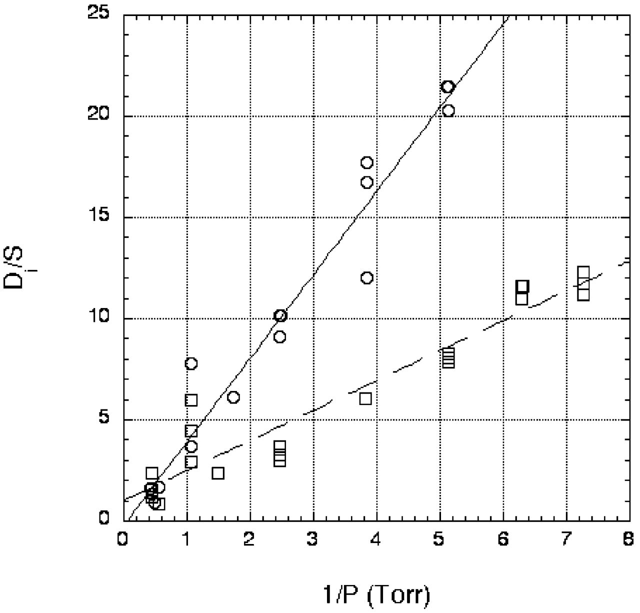

Figure 5. D/S versus reciprocal pressure plot for 2,3-HCl elimination (circles) and 2,3-DCl elimination (squares) of $CF_3CHClCH_3$ and $CF_3CHClCD_3$. The slope is 4.1 ± 0.2 Torr, the intercept is −0.24 ± 0.63, and the correlation coefficient is 0.98 for $CF_3CHClCH_3$; the corresponding values for $CF_3CHClCD_3$ are 1.5 ± 0.2 Torr, 1.04 ± 0.46, and 0.96.

TABLE 2: Summary of Experimental Rate Constants[a,b]

	$CF_2ClCHFCH_3$		$CF_2ClCHFCD_3$	
reaction	Torr	s^{-1}	Torr	s^{-1}
2,3-FH(FD)	0.22 ± 0.01	$(3.1 \pm 0.3) \times 10^6$	0.074 ± 0.003	$(10.2 \pm 1.0) \times 10^5$
1,2-ClF exchange	0.11 ± 0.01	$(1.5 \pm 0.2) \times 10^6$	0.060 ± 0.003	$(8.3 \pm 0.9) \times 10^5$
1,2-ClH	0.059 ± 0.004	$(8.2 \pm 1.0) \times 10^5$	0.038 ± 0.002	$(5.3 \pm 0.6) \times 10^5$
1,2-FH	not observed[c]		not observed[c]	

	$CF_3CHClCH_3$		$CF_3CHClCD_3$	
reaction	Torr	s^{-1}	Torr	s^{-1}
2,3-HCl(DCl)	4.1 ± 0.2	$(5.6 \pm 0.9) \times 10^7$	1.5 ± 0.2	$(2.1 \pm 0.4) \times 10^7$
1,2-FH	not observed[c]		not observed[c]	
1,2-FCl exchange	not observed[c]		not observed[c]	

[a] The listed uncertainties in the rate constants (Torr units) are the standard deviations from the D_i/S vs pressure^{-1} plots. The absolute uncertainty is larger because of uncertainty in the collision diameters (and ϵ/k) and the calibration of the response of the gas chromatograph. Therefore, the uncertainties listed for the rate constants of $CF_2ClCHFCH_3(CD_3)$ in Torr units have been doubled for s^{-1} units. Because the experimental uncertainties were large (±15%) for the $CF_3CHClCH_3$ data, the same uncertainties were used in s^{-1} units. [b] The rate constants in Torr units were converted to s^{-1} using the following collision diameters and ϵ/k values:[13,14] $CF_2ClCHFCH_3$ (5.3 Å and 410 K), $CF_3CHClCH_3$ (5.3 Å and 410 K), CH_3I (4.6 Å and 405 K), and $CF_2ClCHFI$ (5.2 Å and 360 K); $k_M = \pi d^2_{AM} (8kT/\pi\mu_{AM})^{1/2}\Omega^{2,2}(T)^*$. [c] If the reaction was not observed, the rate constant is less than one-eighth of the largest rate constant.

elimination from $CF_3CHClCH_3$ vs 2,3-FH elimination from $CF_2ClCHFCH_3$ is mainly a consequence of the higher energy acquired from the isomerization, reaction 4d. The data of Figure 5 definitively establish Cl−F interchange as an elementary reaction.

The rate constants in pressure units were converted to s^{-1} from calculation of the collision constant, k_M. The collision diameters and ϵ/k values[13,14] used to convert rate constants from Torr units to s^{-1} units are given in footnote *b* of Table 2. The uncertainty in the collision cross sections augments the small experimental uncertainty in the slopes of the D_i/S plots from the $CF_2ClCHFCH_3(CD_3)$ data, and the rate constants in s^{-1} units given in Table 2 show this larger uncertainty. The uncertainties associated with chemical activation rate constants measured in this series of papers dealing with fluorochloropropanes are more fully discussed in refs 1 and 6.

3.2. Thermochemistry. To assign the E_0 values from the rate constants of reactions 4 and 6, the average internal energies of $CF_2ClCHFCH_3(CD_3)$ and $CF_3CHClCH_3(CD_3)$ must be known. The average energy for molecules formed by radical recombination with zero activation energy can be obtained from

$$\langle E(CF_2ClCHFCH_3)\rangle = D_0(CF_2ClCHF{-}CH_3) + 3RT + \langle E_V(CH_3)\rangle + \langle E_V(CF_2ClCHF)\rangle \quad (8)$$

The $3RT$ arises from the 3 translational and 3 rotational motions of the radicals that become vibrational motions in the molecule. The $\langle E_V(CH_3)\rangle$ and $\langle E_V(CF_2ClCHF)\rangle$ terms are the average vibrational energy of the radicals at 298 K. The most important term is the bond-dissociation energy, which is obtained from enthalpies of formation. $\Delta H^\circ_{f,298}(CH_3)$ is well-known (35.0 kcal mol^{-1})[17] and we used isodesmic reactions to estimate $\Delta H^\circ_{f,298}(CF_2ClCHF)$ and $\Delta H^\circ_{f,298}$ $(CF_2ClCHFCH_3)$. The details for the isodesmic reactions are summarized in Table 3. Three different reactions were used for CF_2ClCFH, and they gave similar values for $\Delta H_f(CF_2ClCFH)$; the average value is −118.4 kcal mol^{-1}. Combining this with $\Delta H^\circ_f(CF_2ClCFHCH_3) = -175.5$ kcal mol^{-1} gives $D_{298} = 92.1$ kcal mol^{-1}. Converting to D_0 and using the terms in eq 8 gives $\langle E(CF_2ClCHFCH_3)\rangle = 94.3$ kcal mol^{-1}; the $\langle E(CF_2ClCFHCD_3)\rangle$ increases by 0.3 kcal mol^{-1}. This $\langle E(CF_2ClCHFCH_3)\rangle$ is slightly lower than $\langle E(CF_3CHFCH_3)\rangle^6 = 97$ kcal mol^{-1} formed from $CH_3 + CF_3CHF$; both numbers have uncertainties of 2−3 kcal mol^{-1}.

The average energy of $CF_3CHClCH_3$ formed by reaction 4d is given by

$$\langle E(CF_3CHClCH_3)\rangle = \langle E(CF_2ClCHFCH_3)\rangle - \Delta H^\circ_0(4d) \quad (9)$$

The enthalpy of reaction 4d was calculated as −9.5 kcal mol^{-1} from the Gaussian suite[22] of programs at the B3PW91/6-311+G(2d,p)[4] level and −12.4 kcal mol^{-1} at the B3PW91/6-31G(d′,p′) level in the present work. We gave the larger basis set result more weight and selected −10.5 kcal mol^{-1} for ΔH°_0(4d) and $\langle E(CF_3CHClCH_3)\rangle = 104.8$ kcal mol^{-1}.

In the Discussion the 2,3-FH elimination and Cl−F interchange reactions of $CF_2ClCF_2CH_3$ will be compared with those of $CF_2ClCFHCH_3$. Therefore, $\langle E(CF_2ClCF_2CH_3)\rangle$ formed from $CH_3 + CF_2ClCF_2$ is needed. Isodesmic reactions at the level described in ref 3 were used to obtain $\Delta H^\circ_{f,298}(CF_2ClCF_2CH_3) = -225$ kcal mol^{-1}. McMillen and Golden[20] give $\Delta H^\circ_{f,298}(CF_2ClCF_2) = -164 \pm 4$ kcal mol^{-1} and $D_{298}(CF_2ClCF_2{-}CH_3))$ is 95.7 kcal mol^{-1}. This value is reasonable, because the extra F atom, relative to $CF_2ClCFHCH_3$, would be expected to increase the bond energy. The $\langle E(CF_2ClCF_2CH_3)\rangle$ for $CH_3 + CF_2ClCF_2$ is 98 ± 3 kcal mol^{-1}.

3.3. Assignment of Threshold Energies. In previous work, threshold energies for reactions 4 and 6 were calculated using DFT at the B3PW91/6-311+G(2d,p) level.[4] The E_0 values for 1,2-FH, 1,2-ClH, 2,3-FH, and Cl−F interchange from $CF_2ClCHFCH_3$ were 66.7, 57.6, 59.6, and 55.0 kcal mol^{-1}, respectively. The 9.1 kcal mol^{-1} higher value for 1,2-FH vs 1,2-ClH elimination explains why reaction 4a was not observed in the present work, although these calculated threshold energies are not sufficiently accurate to be used to calculate reliable rate constants.

We have repeated the DFT calculations with the 6-31G(d′,p′) basis set to be in accord with previous calculations[1−3,6] of structural properties of transition states. The calculated threshold energies were 71.2, 56.4, 60.6, and 56.3 kcal mol^{-1} for 1,2-FH, 1,2-ClH, 2,3-FH, and Cl−F interchange, respectively. The order of these E_0 values is the same as from the 6-311+G(2d,p) basis set, but the actual values differ by 1−4 kcal mol^{-1}. The frequencies and moments of inertia were employed to obtain rate constants using the RRKM method, eq 10, with E_0 acting

$$k_E = (s^\ddagger/h)(I^\ddagger/I)^{1/2}(\Sigma P^\ddagger(E - E_o)/N_E^*) \quad (10)$$

TABLE 3: Enthalpy of Formation of $CF_2ClCHFCH_3$ and CF_2ClCHF[a]

	$CF_2ClCHFCH_3 + CH_3F \rightarrow CF_3CHFCH_3 + CH_3Cl$				
total energy[b]	−549, 890.6	−87, 658.7	−323, 790.5	−313, 772.6	$\Delta H^\circ_{RX} = -13.8$
$\Delta H^\circ_{f,298}$[d,e]	(−175.5)	−55.9	−225.6	−19.6	
	$CF_2ClCHF + C_2H_6 \rightarrow \mathbf{CF}_2ClCH_2F + C_2H_5$				
total energy[c]	−524, 829.2	−50, 044.0	−525, 240.6	−49, 632.1	$\Delta H^\circ_{RX} = 0.5$
$\Delta H^\circ_{f,298}$[d,e]	(−120.5)	−20.1	−169.0	28.9	
	$CH_3Cl + CF_3CH_2 \rightarrow \mathbf{CF}_2ClCHF + CH_4$				
total energy[c]	−313, 774.5	−236, 460.4	−524, 829.2	−25, 396.8	$\Delta H^\circ_{RX} = 8.9$
$\Delta H^\circ_{f,298}$[d,e]	19.6	−124.2	(−117.0)	−17.9	
	$C_2H_5Cl + CF_3CH_2 \rightarrow CF_2ClCHF + C_2H_6$				
total energy[c]	−338, 426.1	−236, 460.4	−524, 829.2	−50, 044.0	$\Delta H^\circ_{RX} = 13.3$
$\Delta H^\circ_{f,298}$[d,e]	−26.8	−124.2	(117.6)	−20.1	

[a] All entries are in kcal mol^{-1}. [b] Calculated total electronic energy from B3PW91/G-311++G(2d,p). [c] Calculated total electronic energy from B3PW91/G-311+G(2d,p). [d] Experimentally determined enthalpies of formation. The number in parentheses was deduced from use of ΔH°_{RX}. [e] The ΔH°_f values for CH_3Cl, C_2H_5Cl, and C_2H_6 were taken from ref 18; $\Delta H^\circ_f(C_2H_5)$ is from ref 17, $\Delta H^\circ_f(CF_3CH_2)$ is from refs 19 and 20, and $\Delta H^\circ_f(CH_3F)$ is from ref 21. The ΔH°_f values for CF_3CFHCH_3 and CF_2ClCH_2F were obtained from isodesmic calculations following the examples given in ref 3.

as a parameter to be fitted. We treated the three overall rotations as adiabatic, and the $I^\ddagger/I$ term is the ratio of the principal moments of inertia of the transition state and the molecule. The moments of inertia of the transition states are similar to those of the molecule, and the $I^\ddagger/I$ in eq 10 was 1.3 or smaller for all reactions treated in this paper. The reaction path degenercies, $s^\ddagger$, were 1, 2, 3, and 1 for 1,2-ClH loss, 1,2-FH loss, 2,3-FH loss, and Cl−F interchange, respectively, from $CF_2ClCHFCH_3$ and 3 for 2,3-ClH loss from $CF_3CHClCH_3$. Although two optically active transition states exist for 1,2-ClF interchange, each optically active molecule can access only one transition-state isomer. The sum of states for the transition state and the density of states for the molecule were calculated using hindered internal rotations (HIR) for the torsional modes of the molecules and transition states. The E_0 values were assigned by matching the $k_{\langle E \rangle}$ values to the k(expt) of Table 2 for $\langle E \rangle$ equal to the average energy. The threshold energies for reactions of $CF_2ClCHFCD_3$ and $CF_3CHClCD_3$ can be obtained from the E_0 assigned to $CF_2ClCHFCH_3$ and $CF_3CHClCH_3$ and zero-point energy considerations or from comparison of the calculated $k_{\langle E \rangle}$ values vs the k(expt) for $CF_2ClCHFCD_3$ and $CF_3CHClCD_3$. If the data are self-consistent, both approaches should give the same value for the threshold energy.

The vibrational frequencies and moments of inertia for the molecules and transitions states are provided in the Supporting Information. The asymmetric rotor, CF_2Cl, gives three conformers for $CF_2ClCHFCH_3(CD_3)$ and for the transition state for 2,3-FH(FD) elimination. The calculated absolute energies for the three conformers of the molecule differed by less than 0.3 kcal mol^{-1}. Therefore, the geometric mean of the frequencies and moments of inertia of the three conformers were averaged, and the results were used for calculating the density of states for the molecule in eq 10. Two of the transition-state conformers for 2,3-FH elimination were 2−3 kcal mol^{-1} above the lowest energy conformer. Nevertheless, an average of the conformer frequencies and moments of inertia were used. Actually, the differences among the frequencies of the conformers is small, and the average frequency hardly differs from that of any one conformer. Although the 1,2-FH process was not observed, we did calculations for that pathway. That reaction has two geometric isomers (E and Z) as transition states; their frequencies and moments of inertia were averaged to calculate the sum of states needed in eq 10. The barriers to internal rotation for CF_2Cl in $CF_2ClCHFCH_3$ were estimated using the B3PW91/6−31G(d′,p′) method by locating the tops of the internal rotation barriers as transition states. Fortunately, the barriers (V_{CF_2Cl}) were similar (2.3, 3.0, and 3.2 kcal mol^{-1}) and we treated CF_2Cl as a rotor with three equal barriers. By comparison with other calculations in the literature, we suspect that the calculated barriers are too low, and we used 4.0 kcal mol^{-1} as V_{CF_2Cl}. The calculated barrier for CH_3 was 3.2 kcal mol^{-1}, which is similar to that of other CF_3CXYCH_3 type molecules.[3,23] The CF_3 and CH_3 barriers of $CF_3CHClCH_3$ were assigned as 4.7 and 3.0 kcal mol^{-1} by analogy to similar fluoropropanes.[3,23] The V_{CF_2Cl} and V_{CH_3} for the transition states were taken to be the same as for the molecules. The calculated rate constants are not sensitive to modest changes in barrier heights. For example, the rate constants for free-rotor models were nearly identical to those calculated with hindered rotor models with the barriers just quoted.

Rate constants were calculated using the Multi-Well code generously provided by Professor Barker.[24] This code has a provision for calculating sums and density of states with hindered internal rotors. The reduced moments for internal rotation, I_{red}, were calculated using the method of Pitzer.[25] The CF_2Cl rotor was treated as a symmetric rotor; i.e., the barriers to internal rotation were considered equal and I_{red} values were averaged for the conformers. The I_{red} values are 41.9 and 3.15 amu Å^2 for $CF_2ClCHFCH_3$ and 47.5 and 3.16 amu Å^2 for $CF_3CHClCH_3$; the smaller number is for the CH_3 rotor. The I_{red} for CD_3 increases to 6.21 and 6.24 amu Å^2 for $CF_2ClCHFCD_3$ and $CF_3CHClCD_3$, respectively; the I_{red} for CF_2Cl and CF_3 groups for the deuterated molecules increased by 5−8%. Although the changes relative to the molecules were small, I_{red} were calculated for each transition state.

In addition to RRKM rate constants, thermal pre-exponential factors (in partition function form) were calculated for each reaction channel. These provide an overall measure of the structure of the transition states, relative to their parent molecule. Pitzer's[25] tables were used to calculate the thermal partition functions for the hindered internal rotors. These pre-exponential factors are summarized in Table 4. In general, transition states for ClH elimination have approximately 2-fold larger pre-exponential factors than transition states for analogous FH elimination,[1,3] but the difference between 1,2- and 2,3-elimination[6a] makes the HF and HCl elimination pre-exponential factors nearly equal for $CF_2ClCHFCH_3$. The pre-exponential factor for the ClF interchange reaction is 4 times smaller than that for 1,2-ClH elimination or 2,3-FH elimination.

The threshold energies needed to match the calculated $k_{\langle E \rangle}$ to the experimental rate constants are summarized in Table 4 for $CF_2ClCHFCH_3$ with $\langle E \rangle = 94.3$ kcal mol^{-1}. We expect these

TABLE 4: Comparison of Calculated and Experimental Rate Constants

reaction	k_a(expt)[a]	$\langle E\rangle$[b]	$k_{\langle E\rangle}$[a]	E_0[b]	pre-exp factor,[c] 10^{13} s^{-1}
$CF_2ClCHFCH_3$		94.3			
2,3-FH	31×10^5		28×10^5	59.5	2.20
Cl−F interchange	15×10^5		14×10^5	57.5	0.49
1,2-ClH	8.2×10^5		8.8×10^5	62.5	2.23
1,2-FH	not observed			≥ 69	1.19
$CF_2ClCHFCD_3$		94.6			
2,3-FD	10.2×10^5		9.8×10^5	60.5	2.19
Cl−F interchange	8.3×10^5		8.7×10^5	57.5	0.59
1,2-ClH	5.3×10^5		4.6×10^5	62.5	2.29
1,2-FH	not observed			≥ 69	1.16
$CF_3CHClCH_3$		104.8			
2,3-ClH	5.6×10^7		6.3×10^7	59.0	4.64
Cl−F interchange	($\approx 9.7 \times 10^5$)[e]			(≈ 68)[d]	
1,2-FH	not observed			≥ 67[e]	3.59
$CF_3CHClCD_3$		105.1			
2,3-ClD	2.1×10^7		2.5×10^7	60.0	4.45
Cl−F interchange	($\approx 5.2 \times 10^5$)[e]			(≈ 68)[d]	
1,2-FH	not observed			≥ 69[e]	

[a] In units of s^{-1}. [b] In units of kcal mol^{-1}, assigned by matching k(expt) and $k_{\langle E\rangle}$ for $CF_2ClCHFCH_3$ and $CF_3CHClCH_3$. The E_0 values for $CF_2ClCHFCD_3$ and $CF_3CHClCD_3$ also were obtained from fitting the experimental rate constants. Another method is to use the threshold energies of $CF_2ClCHFCH_3$ and $CF_3CHClCH_3$ plus zero-point energies (see text). [c] Thermal pre-exponential factor at 1000 K in partition function form. To make direct comparisons among the different channels of $CF_2ClCHFCH_3(CD_3)$, the symmetry number for internal rotation of $CH_3(CD_3)$ was maintained as 3 for all calculations with $s^\ddagger$ as 1 for 1,2-ClH, 1,2-FH loss, and ClF interchange. For ease of comparison with 2,3-FH loss from $CF_2ClCHFCH_3$, the internal rotational symmetry numbers for both CH_3 and CF_3 in $CF_3CHClCH_3(CD_3)$ were taken as 3; thus, the pre-exponential factor for 1,2-FH loss from $CF_3CHClCH$, must be divided by 3 for comparison to 1,2-FH loss from $CF_2ClCHFCH_3(CD_3)$. [d] Although 1,2-FCl interchange was not observed, the rate constant was estimated from the rate constants of the forward reaction and the equilibrium constant between the $CF_2ClCHFCH_3(CD_3)$ and $CF_3CHClCH_3(CD_3)$ molecules. E_0 was estimated as $E_0(ClF;CF_2ClCHFCH_3) - \Delta H^\circ_R$. [e] Assigned from the claim that k(1,2-FH) is equal to or less than one-eighth of the k(1,2-ClH) or k(2,3-ClH); see text.

absolute values for E_0(1,2-ClH) = 62.5, E_0(2,3-FH) = 59.5 and E_0(Cl−F) = 57.5 kcal mol^{-1} to be reliable to within ±1.5 kcal mol^{-1}. The basis for the assignment of this uncertainty was given in ref 6. However, the differences between the E_0 values should be more reliable, because they depend only on the branching ratios. The Cl−F exchange reaction has the lowest threshold energy. Because the 1,2-FH reaction was not observed, the rate constant must be ≥8 times smaller than for 1,2-ClH elimination, which sets a lower limit to E_0(1,2-FH) of approximately 69 kcal mol^{-1}; which is consistent with 71.2 kcal mol^{-1} calculated from the 6-31G(d′,p′) basis set.

The experimental rate constants from $CF_2ClCHFCD_3$ first were treated as an independent data set, and E_0 values were assigned to give satisfactory matches between experimental and calculated rate constants for the three observed reaction channels. The assigned E_0 for 2,3-FD elimination is 1.0 kcal mol^{-1} higher than the E_0 for 2,3-FH elimination from $CF_2ClCHFCH_3$. On the basis of the zero-point energies calculated from DFT, the difference should be 1.0 kcal mol^{-1}, and the agreement is excellent for the 2,3-HF(DF) reaction. The fitted E_0 values for 1,2-ClH and 1,2-ClF interchange reactions from $CF_2ClCHFCD_3$ are the same as from $CF_2ClCHFCH_3$. Zero-point energy considerations also predict that the threshold energies for $CF_2ClCHFCH_3$ and $CF_2ClCHFCD_3$ should be identical for these two channels. The kinetic-isotope effects for the 1,2-ClF and 1,2-ClH processes are purely statistical secondary kinetic-isotope effects. The molecular density of states ratio (7.6 at 94 kcal mol^{-1}) is reduced by the sum of states ratio, which is 3.7 and 3.9 at 32 kcal mol^{-1} for 1,2-ClH and 1,2-ClF transition states, respectively. The calculated isotope effects are 1.7 for 1,2-ClH and 1.6 for 1,2-ClF; the experimental rate constant ratios of 1.6 ± 0.3 and 1.8 ± 0.4 are in accord with the calculation. The calculated ratio is nearly the same for both the hindered-rotor and vibrational models, and the calculated ratios are not very sensitive to the detailed structures of the transition states. In this study we have used the $CF_2ClCHFCD_3$ data as independent support for the threshold energies rather than trying to employ kinetic-isotope effects as tests of transition-state structures.

The rate constant for 2,3-ClH elimination from $CF_3CHClCH_3$ also was fitted, and the E_0 value is listed in Table 4. The larger experimental uncertainty for the rate constant of reaction 6 leads us to assign E_0(2,3-ClH) = 59 ± 2 kcal mol^{-1}. The calculated rate constant for 2,3-ClD elimination with a 1.0 kcal mol^{-1} larger E_0 satisfactorily matches the experimental result. According to zero-point energy changes, the difference in threshold energies should be 1.09 kcal mol^{-1}. The similarity of E_0(2,3-FH) from $CF_2ClCHFCH_3$ and E_0(2,3-ClH) from $CF_3CHClCH_3$ is somewhat surprising. Considering the uncertainties in k_{ept}(2,3-ClH), in the calculations and in $\langle E(CF_3CHClCH_3)\rangle$, E_0(HCl) could be lower than 59 kcal mol^{-1}. For example, a reduction in $\langle E(CF_3CHClCH_3)\rangle$ of 2 kcal mol^{-1} would require a 0.5 kcal mol^{-1} reduction in E_0 to have the same k_E. However, the difference between E_0(2,3-FH) and E_0(2,3-ClH) is not large, as demonstrated by the detailed study[3] of $CF_3CClFCH_3$ for which the difference in threshold energies was just 2.8 kcal mol^{-1}. The actual difference in threshold energies for $CF_2ClCHFCH_3$ and $CF_3CHClCH_3$ is probably around 2 kcal mol^{-1}. The 1,2-FH elimination reaction from $CF_3CHClCH_3$ was not observed; however, the threshold energy should be comparable to that for 1,2-FH elimination from CF_3CHFCH_3,[6] which is ≈73 kcal mol^{-1}. The 1,2-FCl interchange rate is very slow relative to 2,3-ClH elimination from $CF_3CHClCH_3$; however, the reverse reaction is only 50−60% slower than reaction 4d because of partial compensation for the energy difference by the effect of the symmetric CF_3 rotor on the density of states of $CF_3CHClCH_3$.

4. Discussion

4.1. Comparison of 1,2-ClF Interchange and 2,3-FH Reactions of $CF_2ClCF_2CH_3$ and $CF_2ClCHFCH_3$. In this section we will compare threshold energies, which requires fitting the experimental rate constants[5] for $CF_2ClCF_2CH_3$ by the same methods used for $CF_2ClCHFCH_3$. Thus, new DFT calculations were done using the 6-31G(d′,p′) basis set. The calculated threshold energies were 64.2 and 65.1 kcal mol^{-1} for ClF interchange and 2,3-FH elimination, respectively; the corresponding values from the 6-311+G(2d,p) basis set[4,5] were 62.5 and 63.8 kcal mol^{-1}. The I_{red} for the HIR models were constructed from the calculated structures. The pre-exponential factors for the reactions of $CF_2ClCF_2CH_3$ were quite similar to those given in Table 4 for $CF_2ClCFHCH_3$. The main difference between the two systems is the higher density of states, because of the additional F atom, for $CF_2ClCF_2CH_3$; see Table 5. The experimental rate constants, adjusted to the collision parameters used in Table 2, for $CF_2ClCF_2CH_3$ are k(1,2-ClF) = 4.3×10^4 and k(2,3-HF) = 6.5×10^5 s^{-1}. Fitting these experimental rate constants for $\langle E\rangle$ = 98 kcal mol^{-1} gives threshold energies of 67 and 65 kcal mol^{-1} for the 1,2-ClF and 2,3-HF channels, respectively. These threshold energies are higher than those from $CF_2ClCHFCH_3$, as expected for transition states with an additional F atom on a carbon atom that is in the four-centered

TABLE 5: Comparison of 2,3-FH Elimination Reactions

molecule	$k_{\langle E\rangle}$(expt), s^{-1}	$\langle E\rangle$, kcal/mol	N^*_{95},[a] states/cm^{-1}	E_0, kcal/mol
CF_3CHFCH_3[b]	3.7×10^6	97	0.96×10^{16}	60.5 ± 1.5
$CF_3CF_2CH_3$[c]	7.7×10^5	98	14×10^{16}	65 ± 2
$CF_3CFClCH_3$[c]	5.6×10^5	94	48×10^{16}	61.3 ± 1.5
$CF_2ClCHFCH_3$[d]	3.1×10^6	94	11×10^{16}	59.5 ± 1.5
$CF_2ClCF_2CH_3$[e]	6.5×10^5	98	156×10^{16}	65 ± 2

[a] Density of states for hindered internal rotor model at 95 kcal mol^{-1} internal energy. Symmetry numbers of 3 for $-CF_3$ and $-CH_3$ rotors are included; the symmetry number for $-CF_2Cl$ is 1. [b] Reference 6. [c] Reference 3. [d] This work. [e] Data from ref 5 with $k_{\langle E\rangle}$(expt) adjusted to the collision cross sections used in the present work; E_0 was assigned in this work.

ring[6a] or on a C atom that is part of the bridged transition state. Just as for $CF_2ClCHFCH_3$, the DFT calculated threshold energy for ClF interchange for $CF_2ClCF_2CH_3$ is slightly below the experimental value. The calculated E_0(2,3-FH) values, for the lowest energy conformer of the transition state, are close to the experimental values for both molecules. The largest discrepancy between the experimental and calculated threshold energies is for 1,2-HCl elimination.

We also took this opportunity to use the molecular and transition-state structures from the 6-311+G(2d,p) basis set to calculate RRKM rate constants for $CF_2ClCF_2CH_3$. These rate constants differed by less than 15% from those described above and the assigned E_0(1,2-ClF) and E_0(2,3-FH) would be unchanged. This comparison supports previous claims that rate constant calculations[1,3] are not very sensitive to the basis set used to obtain structures of the transition states.

The rate constants, density of states, and threshold energies for 2,3-HF elimination of several fluoropropane molecules are summarized in Table 5. The density of states increases as heavy atoms are added to the molecules, but this effect on the rate constants is partly counterbalanced by an increase in the sum-of-states for the transition state. Providing that the internal rotation modes are similar, the net effect on the overall ratio is a factor of 1.7 for exchange of one H atom by a F atom and 2.0 for exchange of one H atom by a Cl atom, and the main factor that determines k_E is still the threshold energy. On the basis of the $CF_3CHFCH_3-CF_2ClCHFCH_3$ and $CF_3CF_2CH_3-CF_2ClCF_2CH_3$ pairs, the substitution of a Cl atom for a F atom in the CF_3 group does not change the E_0 for 2,3-HF elimination. However, the threshold energies for $CF_3CF_2CH_3$ and $CF_3CFClCH_3$ are not equal, and the effect of a Cl atom in the secondary position is similar to that of the H atom in CF_3CHFCH_3.

4.2. Nature of ClF Interchange Reactions. The observation of $CF_3CHClCH_3$ from reaction 4d proves the 1,2-Cl−F interchange mechanism for $CF_2ClCFHCH_3$. The observed final products also are convincing evidence for 1,2-Cl−F interchange in $CF_2ClCF_2CH_3$,[4,5] CF_3CH_2Cl,[10,12] and CF_2HCH_2Cl.[10,11] The transition state for Cl−F interchange is a double-bridged structure with the F and Cl atoms nearly equidistant from each C atom; see Figure 1. The C−F distances are 1.85 and 1.79 Å, for carbon atoms 1 and 2, respectively, and the corresponding C−Cl distances are 2.38 and 2.36 Å. The geometry around the two carbon atoms is quasi planar, and the carbon atoms have nearly sp^2 geometry with a C−C distance that is midway between that of the parent molecule and the product olefin. The transition-state structure from the 6-311+G(2d,p) basis set was nearly identical to that from the 6-31G(d′,p′) basis set. One way of thinking about the transition state is to imagine the simultaneous free-radical addition of one Cl atom and one F atom to $CF_2{=}CHCH_3$. Although the C−F and C−Cl bonds in the transition state are extended by about 50% relative to the $CF_2ClCHFCH_3$, the entropy of activation is −1.3 cal mol^{-1} K^{-1} at 800 K for the HIR model, and the transition-state structure is relatively rigid.

We also searched for ClF interchange in some ethane and propane molecules containing only fluorine and chlorine atoms.[26] Vibrationally excited $CF_2ClCF_2CF_3$, $CF_2ClCF_2CF_2Cl$, and CF_2ClCF_2Cl molecules were generated by (i) photolysis of $(CF_2Cl)_2CO$, (ii) co-photolysis of $(CF_3)_2CO$ with CF_2ClCF_2I, and (iii) co-photolysis of CF_3I with CF_2ClCF_2I. Experiments were done over the $(0.21-1.1) \times 10^{-4}$ Torr range of pressure. The expected radical recombination products were observed at high pressure. However, no evidence was found for molecules formed by Cl−F interchange. At the lowest pressures, the total number of products increased, and C−Cl bond rupture probably was occurring. Apparently, the threshold energy for Cl−F interchange is quite high for these three molecules. DFT calculations[27] for CF_2ClCF_2Cl at the B3PW91/6-311+G(2d,p) level gave 70.4 kcal mol^{-1} as the threshold energy for CF_3CFCl_2 formation, and the true value may be even higher. For these three molecules, ClF interchange is not competitive with C−Cl bond rupture for $\langle E\rangle \approx 95$ kcal mol^{-1}.

On the basis of the somewhat limited number of examples, the variation of the threshold energies for ClF interchange with substituents on carbon atoms 1 and 2 seems to follow those for HF or HCl elimination.[6] That is, the presence of H atoms or CH_3 groups on the carbon atoms in the bridge seems to lower the threshold energy for interchange. A systematic computational investigation[27] of threshold energies for $C_2H_xF_yCl_z$ molecules shows that Cl−F interchange usually needs to be included as one of the possible competing unimolecular reactions.

4.3. Comparison of Transition States for 1,2-FH and 1,2-ClH Elimination Reactions. A previous study[6] of CF_3CHFCH_3 demonstrated that the pre-exponential factor is a factor of 2 larger for 1,2-FH elimination than for 2,3-FH elimination, which corresponds to a higher entropy (1.4 cal mol^{-1} K^{-1}) for the 1,2-FH transition state. This is somewhat counter intuitive given the presence of a CF_3 internal rotor in the 2,3-FH transition state versus a CH_3 rotor in the 1,2-FH transition state. However, the 1,2-FH transition state has low bending frequencies associated with the CF_2 group in proximity to the F atom in the four-membered ring. The ≥10 kcal mol^{-1} higher E_0(1,2-FH) ensures that 2,3-FH elimination is still the dominant reaction path. Transition states for HCl elimination generally have larger pre-exponential factors than HF elimination, if all other factors are constant,[1,3] and the calculated pre-exponential factors for $CF_3CHClCH_3$ in Table 4 show that 2,3-ClH elimination is favored by both the pre-exponential factor and the low threshold energy. The 1,2-FH and 1,2-ClH processes are in competition for $CF_2ClCHFCH_3$ and, as expected, the transition state for ClH elimination is less rigid with a 2-fold larger pre-exponential factor. The pre-exponential factor for the overall 2,3-FH elimination becomes comparable to that for 1,2-ClH elimination for $CF_2ClCHFCH_3$ as a consequence of the presence of the CF_2Cl rotor for 2,3-elimination. Because threshold energies are intrinsically lower for 2,3-XH than 1,2-X′H elimination from CX'_3CHXCH_3 type molecules, $CF_2ClCHFCH_3$ is an unusual example for which HF elimination is dominant over HCl elimination.

The experimentally assigned value for E_0(1,2-ClH) is 62.5 kcal mol^{-1}, which is ≈5 kcal mol^{-1} higher than the DFT calculated value from either basis set. The calculated values are only 2−3 kcal mol^{-1} higher than the E_0 for CH_3CH_2Cl, which seems too low given the presence of three out-of-ring F atoms in the 1,2-HCl elimination transition state for $CF_2ClCHFCH_3$.[6] Because reaction 4a was not actually observed, E_0(1,2-FH) could not be experimentally assigned. On the basis of a limit of k(1,2-FH) $\leq$ $^1/_8k$(1,2-ClH), the E_0(1,2-FH) must be $\geq$69 kcal mol^{-1}. This estimate would place the threshold energy close to the DFT calculated values, which also are typical for 1,2-FH elimination from CF_3CH_2R (R = X or CH_3) type molecules.[6] The DFT calculations are usually more reliable for threshold energies of HF elimination than for HCl elimination.[1,6]

In principle a comparison of threshold energies between $CF_2ClCHFCH_3$ and CF_2ClCH_3 should be illustrative. Unfortunately, the published results for CF_2ClCH_3 are not self-consistent,[7,28−30] although the dominance of HCl elimination with a lower threshold energy can be accepted. Thermal activation studies are complicated by a chain reaction. The most recent study,[28] which modeled the simultaneous unimolecular HCl loss and the radical reactions, favored E_a(HCl) = 55.3 kcal mol^{-1}. However, earlier work,[29] which tried to eliminate the radical chain complication, gave E_a(HCl) = 60 kcal mol^{-1}, and an unpublished work[30] gave E_a(HCl) = 69 kcal mol^{-1}. Two chemical activation studies have been reported.[7,30] The early study[30] gave E_0 = 65 kcal mol^{-1} for the favored channel (which they misidentified as HF elimination). A later[7] study claimed E_0(HCl) = 55 kcal mol^{-1}. The experimental rate constants reported in these two studies differ by an order of magnitude, and an independent study will be required to resolve the question of E_0(HCl) for CF_2ClCH_3. On the basis of the current work with $CF_2ClCHFCH_3$, a threshold energy near 60 kcal mol^{-1} would be anticipated.

5. Conclusions

The unimolecular reactions of $CF_2ClCHFCH_3(CD_3)$ molecules with 94.3 kcal mol^{-1} of vibrational energy are 2,3-FH elimination, 1,2-ClF interchange, and 1,2-ClH elimination. The $CF_3CHClCH_3(CD_3)$ molecules formed by the interchange subsequently undergo 2,3-ClH(ClD) elimination or collisional stabilization. The vibrational frequencies and moments of inertia of the molecules and transition states were obtained from DFT calculations with the B3PW91/6-31G(d′,p′) method. Matching RRKM calculated rate constants to experimental values gives threshold energies of 59.5, 57.5, and 62.5 kcal mol^{-1} for the HF, ClF, and HCl channels, respectively, with an uncertainty of ±1.5 kcal mol^{-1}. The kinetic-isotope effects for $CF_2ClCHFCD_3$ support these threshold energy assignments. A summary is provided for 2,3-FH elimination reactions from five fluorochloropropane molecules. The threshold energy for 2,3-ClH elimination from $CF_3CHClCH_3$ is 59 ± 2 kcal mol^{-1}. Results soon to be published[31] for chemically activated $CF_2ClCHFC_2H_5(C_2D_5)$ show the same pattern for unimolecular rate constants as summarized above for $CF_2ClCHFCH_3(CD_3)$. All of these results, plus previous work with $CF_2ClCF_2CH_3(CD_3)$, firmly establish the ClF interchange process as an elementary reaction that can be competitive with HCl and HF elimination reactions for halogenated alkanes with Cl and F atoms on adjacent carbon atoms. Fully halogenated fluorochloroethanes and propanes seem to have high threshold energies for Cl−F interchange, and other decomposition pathways are favored over Cl−F interchange.

According to the DFT calculations, the transition state for ClF interchange is a double-bridged structure with the F and Cl atoms above/below the plane of the carbon backbone. The F and Cl atoms are approximately equidistant from each carbon atom; the C−C distance is about 0.11 Å shorter in the transition state than in the parent alkane. This somewhat resembles the halogen atom migration process for halogenated alkyl radicals.[32−37] The DFT calculations at the B3PW91/6-31G(d′,p′) or /6-311+G(2d,p) levels underestimate the threshold energy for 1,2-ClF interchange, but only by 2−4 kcal mol^{-1}.

Acknowledgment. Financial support for this work was provided by the U.S. National Science Foundation under grants CHE-0239953 and MRI-0320795. We thank Mr. Brian Winslett for permission to quote the studies of CF_2ClCF_2Cl and $CF_2ClCF_2CF_3$ and Mr. Jason Batchelor for his preliminary work with the $CF_2ClCHFCH_3$ and $CF_2ClCHFCD_3$ systems.

Supporting Information Available: Table S1 contains frequenices and moments of inertia computed for the reactants and transition states for $CF_2ClCFHCH_3$ and $CF_3CHClCH_3$ and this material is available free of charge via the Internet at http://pubs.acs.org.

References and Notes

(1) Ferguson, J. D.; Johnson, N. L.; Kekenes-Husker, P. M.; Everett, W. C.; Heard, G. L; Setser, D. W.; Holmes, B. E. *J. Phys. Chem. A* **2005**, *109*, 4540. The question of the value of the threshold energy for $CF_3CH_2CH_3$ has been resolved in favor of a higher value near 68−69 kcal mol^{-1}; see ref 6a.

(2) Roach, M. S.; Sibila, B. M.; Holmes, B. E. *J. Phys. Chem. A*, to be submitted.

(3) Zhu, Li; Simmons, J. G., Jr.; Burgin, M. O.; Setser, D. W.; Holmes, B. E. *J. Phys. Chem. A* **2006**, *110*, 1506.

(4) Heard, G. L.; Holmes, B. E. *J. Phys. Chem.* **2001**, *105*, 1622.

(5) Burgin, M. O.; Heard, G. L.; Martell, J. M.; Holmes, B. E. *J. Phys. Chem.* **2001**, *105*, 1615.

(6) (a) Holmes, D. A.; Holmes, B. E. *J. Phys. Chem. A* **2005**, *109*, 10726. (b) The calculated rate constant for 1,2-FH elimination listed in Table 2 for CF_3CHFCH_3 should be 2.8 × 10^4 s^{-1}, and the calculated kinetic-isotope effect for CF_3CHFCD_3 is 2.2, as quoted in the text.

(7) Jones, Y.; Holmes, B. E.; Duke, D. W.; Tipton, D. L. *J. Phys. Chem.* **1990**, *94*, 4957.

(8) Martell, J. M.; Beaton, P. T.; Holmes, B. E. *J. Phys. Chem. A* **2002**, *106*, 84871.

(9) Clark, W. G.; Setser, D. W.; Dees, K. *J. Am. Chem. Soc.* **1971**, *93*, 5328.

(10) Beaver, M. R.; Heard, G. L.; Holmes, B. E. *Tetrahedron Lett.* **2003**, *44*, 7265.

(11) Dolbier, W. R., Jr.; Romelaer, R.; Baker, J. M. *Tetrahedron Lett.* **2002**, *43*. 8075.

(12) (a) Heard, G. L.; Holmes, B. E. To be published. (b) Smith, S. R.; Holmes, B. E. *Int. J. Chem. Kinet.* **1999**, *31*, 237.

(13) Hippler, J. H.; Troe, J.; Wendelken, H. J. *J. Chem. Phys.* **1983**, *78*, 6709.

(14) Mourits, F. M.; Rummems, F. H. A. *Can. J. Chem.* **1977**, *55*, 3007.

(15) Richmond, G.; Setser, D. W. *J. Phys. Chem.* **1980**, *84*, 2699.

(16) Marcoux, P. J.; Setser, D. W. *J. Phys. Chem.* **1978**, *82*. 97.

(17) Berkowitz, J.; Ellison, G. B.; Gutman, D. *J. Phys. Chem.* **1994**, *98*, 2244.

(18) Kerr, J.A.; Stocker, D. W. Standard Thermodynamic Propertioes of Chemical Substances. In *Handbook of Chemistry and Physics*; Linde, D. R., Jr., Ed.; CRC Press; Boca Raton, FL, 2002.

(19) Zachariah, M. R.; Westmoreland, P. R.; Burgess, D. R., Jr.; Tsang, W.; Melius, C. F. *J. Phys. Chem.* **1996**, *100*, 8737.

(20) McMillen, D. F.; Golden, D. M. *Annu. Rev. Phys. Chem.* **1982**, *33*, 493.

(21) Smith, D. W. *J. Phys. Chem. A* **1998**, *102*, 7086.

(22) Frisch, M. J.; Trucks, G. W.; Schlegel, H. B.; Scuseria, G. E.; Robb, M. A.; Cheeseman, J. R.; Montgomery, J. A., Jr.; Vreven, T.; Kuden, K. N.; Burant, J. C.; Millam, J. M.; Iyengar, S. S.; Tomasi, J.; Barone, V.; Mennucci, B.; Cossi, M.; Scalmani, G; Bega, N; Petersson, G. A.; Nakatsuji, H.; Hada, M.; Ehara, M.; Toyota, K.; Fukuda, R.; Hasegawa, J.; Ishida, M.; Nakajima, T; Honda, Y.; Kitao, O.; Adamo, C.; Jaramillo, J.; Gomperts, R.; Stratman, R. E.; Yazyev, O.; Austen, A. J.; Cammi, R.; Pomelli, C.; Ochterski, J. W.; Ayala, P. Y.; Morokuma, K.; Voth, G. A.; Salvador, P.; Dannenberg, J. J.; Zakrzewksi, V. G.; Dapprich, S.; Daniels, A. D.; Strain, M. C.; Farkas, O.; Malik, D. K.; Rabuck, A. D.; Raghavachari, K.; Foresman, J. B.; Ortiz, J. V.; Cui, Q.; Baboul, A. G.; Clifford, S.; Cioslowski, J.; Stefanov, B. B.; Liu, G.; Liashenko, A.; Piskorz, P.; Komaromi, I.;

Martin, R. L.; Fox, D. J.; Keith, T. Al-Laham, M. A.; Peng, C. Y.; Nanayakkara, A.; Challacombe, M.; Gill, P. M. W.; Johnson, B.; Chen, W.; Wong, M. W.; Gonzalez, C.; Pople, J. A. *Gaussian 03*, revision B.04; Gaussian, Inc., Pittsburg, PA, 2003.

(23) Yamada, T.; Lay, T. H.; Bozzelli, J. W. *J. Phys. Chem. A* **1998**, *102*, 7286.

(24) Barker, J. R. *Int. J. Chem. Kinet.* **2001**, *33*, 232.

(25) (a) Pitzer, K. S.; Gwinn, W. D. *J. Chem. Phys.* **1942**, *10*, 428. (b) Pitzer, K. S. *J. Chem. Phys.* **1946**, *14*, 239.

(26) Winslett, B.; Holmes, B. E. Unpublished work, 2003.

(27) Everett, W. C.; Heard, G. L.; Holmes, B. E. Unpublished work, 2006.

(28) Huybrechts, G.; van Assche, G.; van der Auwera, S. *Int. J. Chem. Kinet.* **1998**, *30*, 359.

(29) Martens, G. I.; Godfroid, M.; Decelle, R.; Verbeyst, J. *Int. J. Chem. Kinet.* **1972**, *4*, 645.

(30) (a) Cadman, P.; Kirk, A. W.; and Trotman-Dickenson, A. F. *J. Chem. Soc. Faraday Trans. 1* **1976**, *72*, 996. (b) Phillips, D. C.; Trotman-Dickenson, A. F. *J. Chem. Soc. A* **1968**, 1667.

(31) Beaver, M. R.; Simmons, J. G., Jr.; Heard, G. L.; Setser, D. W.; Holmes, B. E. *J. Phys. Chem. A*, to be submitted.

(32) Skell, P. S.; Traynham, T. G. *Acc. Chem. Res.* **1984**, *17*, 160.

(33) Engels, B.; Peyerimhoff, S. D.; Skell, P. S. *J. Phys. Chem.* **1980**, *94*, 1267.

(34) Ihee, H.; Zewail, A. H.; Goddard, W. A. III. *J. Phys. Chem. A* **1999**, *103*, 6638.

(35) Knyazev, V. D.; Kalinovski, I. J.; Slagle, I. R. *J. Phys. Chem. A* **1999**, *103*, 3216.

(36) Braña, P.; Menéndez, B.; Fernandez, T.; Sordo, J. A. *Chem. Phys. Lett.* **2000**, *325*, 653.

(37) Ihee, H.; Hua, J.; Goddard, W. A., III.; Zewail, A. H. *J. Phys. Chem. A* **2001**, *105*, 3623.